JOURNAL OF PROPULSION AND POWER
Vol. 27, No. 1, January–February 2011

Theoretical Investigation of the Dynamics of a Gas–Liquid Coaxial Swirl Injector

Qing-fei Fu* and Li-jun Yang†
Beijing University of Aeronautics and Astronautics, 100191 Beijing, People's Republic of China

DOI: 10.2514/1.B34004

In this paper, a linear dynamic characteristics model of a gas–liquid coaxial swirl injector is developed by dividing the injector into two parts: the recessed chamber and the section before the recessed chamber. The gaseous injector flow before the recessed chamber is considered to be steady; only the response of the mass flow rate at the exit of coaxial injector to the pressure fluctuation at the liquid injector inlet has been investigated. The dynamic characteristics of the coaxial swirl injector can now be considered as two processes: the dynamics of the liquid swirl injector and the dynamics of the recessed chamber. The transfer function of the whole injector is obtained by combining the transfer functions of these two processes. The influence of the injector configuration and working condition on the injector dynamic characteristics was also studied. A smaller mixing ratio, larger mass flow rate, higher ambient pressure, smaller ratio of recess length to diameter, and larger geometry parameter would decrease the amplitude response of the mass flow rate pulsation, but these parameters have little effect on the phase frequency of the coaxial swirl injector.

I. Introduction

BIPROPELLANT coaxial injectors are widely used in the liquid propellant rocket engine (LPRE), especially in liquid oxygen (LOX)/hydrogen rocket engines. Coaxial injectors can be classified into shear coaxial injectors and swirl coaxial injectors, according to the spraying mechanism. For a coaxial swirl injector (Fig. 1), LOX is injected with low velocity through a center swirl injector and gaseous hydrogen is injected with high velocity through an annular gap around the center injector. The swirl causes the LOX sheet to have a hollow cone shape, which impinges on the surrounding hydrogen stream; providing better atomization and higher performance. It has been reported that recessing the inner LOX injector (with respect to the exit surface of the outer hydrogen injector), leads to performance enhancement of LPRE [1]. There have been many studies on the spray and combustion characteristics of the coaxial swirl injector with the recess configuration [2–6], however, the dynamic characteristics of this type of injector have been less studied.

The dynamic characteristics of the recessed chamber are of significant importance to the entire coaxial swirl injector. Three different flow models were used for the recessed mixing chamber [7]: the outer mixing flow condition, the inner mixing flow condition and the critical recess flow condition. The gas–liquid interaction in the recessed chamber is very complicated, especially under the inner mixing flow condition (Fig. 2). Hence, it is necessary to study the dynamic characteristics of the coaxial swirl injector under the inner mixing flow condition.

Bazarov [8] reported that during fire tests at 50–75% of nominal thrust level of LOX/LH_2 LPRE, high frequency pressure pulsations appeared in the oxidizer collector of the main combustion chamber, with amplitude up to 0.9 MPa, accompanied by destructive vibrations, with acceleration up to 500–800 g. The origin of these pulsations cannot be explained by the acoustic characteristics of the combustion chamber, because these frequencies were much different from those observed; this phenomenon is called self-pulsation. The reason for the occurrence of self-pulsation may be the hydraulic instability of the conical liquid sheet and the momentum transfer of kinetic energy between the high speed gas stream and liquid sheet in the recessed chamber [9]. Because the liquid sheet emanates from the center swirl injector with a specific spray angle, the annular gas stream is blocked by the conical liquid sheet. The gas stream then pushes the liquid sheet into the centerline, and the liquid and gas phase violently exchange the momentum. When self-pulsation occurs, a loud "scream" and strong flow rate oscillation follow. Such self-pulsation motion was discovered in all types of injectors used in LPRE, such as the shear coaxial injector, coaxial swirl injector with central LOX and exterior hydrogen stages, and both swirl/swirl coaxial injector with central liquid flow, etc.

To understand the mechanism of the unsteady self-pulsation phenomenon and to eliminate the instability, the dynamic characteristics of the gas–liquid coaxial injector were first studied by Andreyev et al. [10,11]. Andreyev studied the dynamic characteristics of the gas–liquid injector and the effect of injector dynamics on the entire LPRE dynamic system. The theoretical study was based on fundamental fluid mechanics' equations and the diagram method, which reveals the interrelation of the dynamic process. Experimental methods were also introduced. Nonlinear dynamics, emphasizing the interaction of the gas and liquid phase, the stability boundary of self-pulsation and the effect of injector geometry on the self-pulsation, were also discussed [10].

Bazarov and Yang [12] performed several experimental studies on the influences of operating conditions and design parameters on the occurrence of self-pulsation. According to his results, the LOX postrecess length is the most important parameter in determining self-pulsation characteristics. Im and Yoon [9] investigated self-pulsation characteristics of a gas/liquid swirl coaxial injector by measuring spray patterns, spray oscillation characteristics, and the self-pulsation boundary. Using indirect photography, they observed strong and periodic spray oscillations. The spray patterns varied at various injection, geometric, and ambient pressure conditions. The main conclusion of their experiments is that: the increase of the ambient pressure suppresses self-pulsation by decaying the dominant wave of the liquid sheet; recess is found to strengthen self-pulsation because the interaction between the liquid and gas phases becomes more active as the recess length increases.

A strong flow rate oscillation is accompanied by the instability phenomenon, or self-pulsation, in a swirl coaxial injector; there is a close relationship between the fluctuation of the injected propellant mass flow rate and the fluctuation of heat release. Therefore, the aim of this study is to develop a simplified method for calculating the dynamic characteristics of a coaxial swirl injector, and to investigate the influences of the injector configuration and working conditions

Received 6 May 2010; revision received 5 September 2010; accepted for publication 13 September 2010.

*Ph.D. Candidate, School of Astronautics.
†Professor, School of Astronautics; yanglijun@buaa.edu.cn (Corresponding Author).

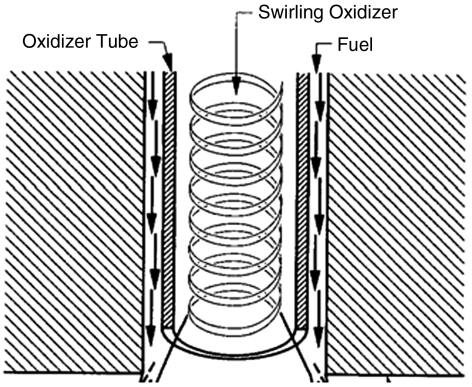

Fig. 1 Schematic of a coaxial swirl injector.

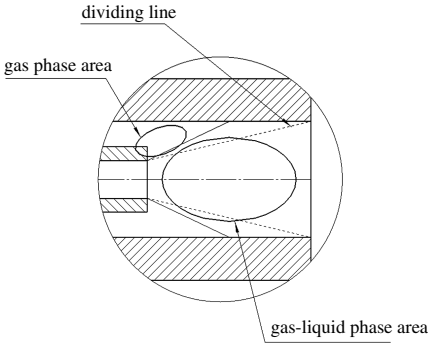

Fig. 2 Schematic of the inner mixing flow condition.

on the dynamics. This paper will emphasize the fluctuation of the mass flow rate of the gas–liquid injector caused by pressure fluctuation in the liquid propellant supply line.

II. Linear Dynamics of Recessed Gas–Liquid Coaxial Swirl Injector

The configuration, as shown in Fig. 3, is a conventional gas–liquid coaxial swirl injector. In Fig. 3, liquid propellant comes to the swirl chamber through the tangential inlet, located at the swirling chamber wall; it forms a swirling flow, and is injected to the nozzle post located at the center of the coaxial swirl injector. Gaseous propellant is supplied through the annular gap between the recessed chamber wall and liquid injector. The exit surface of the inner liquid injector is located at a certain length on the inward side from the exit surface of the outer injector. Section 1-1 is at the tangential inlet of the liquid swirl injector, sections 2-2 and 3-3 are defined as the inlet and outlet of the recessed chamber, respectively. The diameter and length of the recessed chamber are d_R and l_R. The diameters of the tangential inlet, swirl chamber and spout orifice for the liquid swirl injector are d_t, d_k, and d_0 respectively.

Figure 4 shows the dynamic map of a recessed gas–liquid coaxial swirl injector. During internal mixing, the pressure fluctuations of the combustion chamber affect the recessed chamber through the feedback coupling 10, and consequently, the liquid and gas stages of

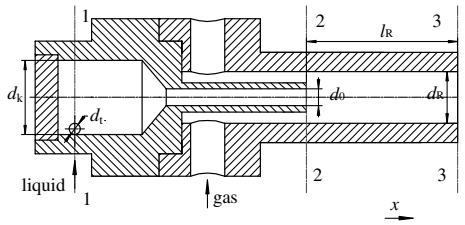

Fig. 3 Schematic of a gas–liquid coaxial swirl injector with recessed chamber.

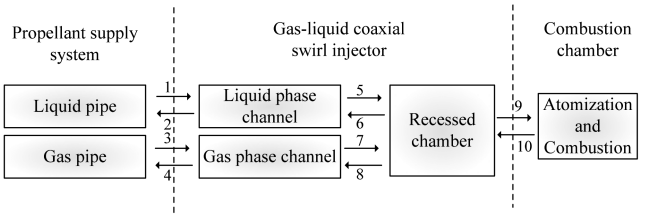

Fig. 4 Interaction of dynamic processes in a recessed gas–liquid coaxial swirl injector.

the injectors (through couplings 6 and 8, respectively). The propellant supply system responds to these disturbances (2 and 4), and generates a flow fluctuation which, when passing through the injector (1-5-9, 3-7-9), results in fluctuations of droplet mass and size distributions of the combustible mixture spray. Feedback coupling 6 can form its own self-pulsation circuits, causing fluctuations in the propellant flow at the injector exit [12]. In the current study, it is assumed that there is pressure fluctuation only at the liquid flow tangential inlet; before coming into the recessed chamber, the gaseous flow is stable. Furthermore, Bazarov [8] reported that chamber pressure pulsation Pc' in the self-pulsation case were sufficiently weaker and did not exceed $10\%Pc$. Therefore, the pressure at the exit of the coaxial swirl injector is assumed to be constant, and only the dynamic route of the liquid phase (1-5-9-6) is studied. To study its dynamics, a recessed coaxial swirl injector can be divided into two components: the liquid swirl injector and the recessed chamber.

A. Linear Dynamic Characteristics of the Recessed Chamber

The following assumptions were made before the study:

1) The breakup length of the liquid sheet is ignored and the gas–liquid two-phase flow in the recessed chamber is regarded as homogeneous flow, i.e., the droplets and the gas phase are uniformly distributed in the recessed chamber. Under the action of centrifugal force, the liquid spreads out in the form of a conical sheet as soon as it leaves the central swirl injector. In the recessed chamber, the velocity of the gas is much higher than the velocity of the liquid phase. The liquid sheet disintegrates under the action of the gas flow. Considering the inner mixing flow condition affirmed by the author [7], the recessed length is large enough so that the swirling liquid sheet will touch the inner surface of the outer gas port, and the gas–liquid phase area will occupy a large section of the recessed mixing chamber. In this case, the outer gas flow and the inner liquid sheet mainly interact in the recessed mixing chamber, and the flow is referred to as an inner mixing flow. Because both the gas flow and the inner surface of the outer port will act on the inner swirl liquid film and contribute to atomization, we assume the primary atomization is accomplished in a very short distance and the liquid sheet is disintegrated into numbers of fragments and droplets. The liquid droplets disperse in the gas flow uniformly and pass through the recessed chamber with the gas phase. This assumption can be verified to some extent by analyzing the spray pattern observed in experiments [4,13], where it was shown that the spray presents the shape of a fully developed cone when the coflow gas is introduced, without recess. When the center injector recessed, the liquid sheet blocking the annular passage was blown off in the shape of a mushroom. The spray cone does not form until the gas–liquid mixture moves downstream for a distance. This indicates that the gas phase and liquid phase mix together in the recessed chamber. If the gas and liquid phase separate from each other, the spray cone would form immediately when they exit the spout exactly as occurs without the recess. The literature [14] also states: “For the developed flow pattern, mixing of the liquid and gaseous jet were promoted and the mixture flow occupied the recessed region. Therefore, only the mixture flow was injected from the injector exit.” Based on the preceding analysis, we think the homogeneous flow assumption can be used in the dynamic analysis for the recessed chamber, at least in the inner mixing condition.

2) Because the viscous force is considerably small compared with the inertial force in the present study (Reynolds number is large), the flow in the recessed chamber is considered to be inviscid. For example, a back-of-the-envelope calculation for an O/F (LOX/GH_2) ratio of eight and a total mass flow rate of 0.3 kg/s gives an average velocity of 57 m/s and the equivalent density for the mixture is about 126 kg/m^3. Hence, the equivalent Reynolds number is about 4×10^5 ($\mu_{LOX} = 1.46e-4$ kg/m · s, $\mu_{H2} = 8.99e-6$ kg/m · s [15]). A large Reynolds number means that the viscous force is considerably small and can be ignored.

3) The flow is one dimensional. Because the cross-sectional area of the recessed chamber is constant and the radial velocity is much smaller compared with the axial velocity, only the axial movement is considered.

4) Since the viscous can be negligible, there is no friction pressure drop. The pressure drop mainly contributes to the accelerating of the fluid column.

The mass flow rate of the two-phase mixture in the recessed chamber is M, and the density of the two-phase mixture is $\rho = \rho_g\beta + \rho_l(1-\beta)$, where ρ_l, ρ_g are the density of the liquid and gas, respectively, and β is the volumetric fraction of the gas phase. Because the flow is considered to be inviscid, the viscous term is neglected and the momentum equation in the recessed chamber can be written as

$$\frac{\partial v}{\partial t} + v\frac{\partial v}{\partial x} = -\frac{1}{\rho}\frac{\partial p}{\partial x} \tag{1}$$

where v is the velocity of the two-phase mixture, p denotes the pressure. Equation (1) is actually the Eulerian equation of motion, which applies to both the compressible and incompressible fluid.

For the reason of inviscid flow, the axial gradient for the velocity in Eq. (1) can be neglected, i.e., $\frac{\partial v}{\partial x}$ can be neglected [15]. Then $\frac{\mathrm{d}v}{\mathrm{d}t} = \frac{\partial v}{\partial t}$, Eq. (1) transforms into

$$\frac{\mathrm{d}v}{\mathrm{d}t} + \frac{1}{\rho}\frac{\partial p}{\partial x} = 0 \tag{2}$$

Integrating Eq. (2) along x direction, the pressure drop in the recessed chamber can be obtained:

$$p_2 - p_3 = \frac{l_R}{S}\frac{\mathrm{d}M}{\mathrm{d}t} \tag{3}$$

Where the mass flow rate $M = \rho S v$, S is the sectional area of recessed chamber. Equation (3) can also be found in section 3.2.2 of Harrje and Reardon's report [16].

It is easier to study dynamic characteristics with a frequency-domain analysis than with a time-domain analysis method. The frequency response equation can be obtained by transforming the fluid mechanics equation with a Laplace transform.

Linearize Eq. (3) and the fluctuation parameter is normalized by the mean variables:

$$\overline{\Delta p}' = \frac{M l_R}{\Delta p S} s\bar{M}' \tag{4}$$

Where $s = j\omega$ is the Laplace operator, $\omega = 2\pi f$ is the angular frequency, $\Delta p = p_2 - p_3$, overbar $-$ denotes the relative quantity, and $'$ denotes the perturbation quantity.

According to the conservation of mass, the relation $M = \rho S v$ holds. Because the sectional area of recessed chamber is constant, the following equation can be obtained:

$$M' = Sv\rho' + \rho S v' \tag{5}$$

Assuming liquid density is constant, $\rho' = \beta\rho_g'$ (the gas phase volumetric fraction β is so large that the variation of gas volumetric fraction caused by the variation of the liquid mass flow rate can be neglected). $v' = \frac{1}{S\rho_l}\dot{m}_l'$ is obtained by the assumption that the gaseous flow before coming into the recessed chamber is stable, where $\dot{m}_l'$ is the perturbation quantity of the liquid mass flow rate, v is the velocity of two-phase uniform flow.

Then the relative perturbation quantity of mass flow rate of the two-phase flow can be expressed as

$$\bar{M}' = \frac{\beta\rho_g'}{\rho} + \frac{1}{Sv\rho_l}\dot{m}_l' \tag{6}$$

And the flow in the recessed chamber is assumed to be isentropic:

$$\rho_g' = \frac{p'\rho_g}{p\gamma} \tag{7}$$

where γ is the ratio of specific heat of two-phase mixture. Because the pressure at the exit of the coaxial swirl injector is assumed to be constant, Eq. (7) can be written in this form [17]:

$$\rho_g' = \frac{\Delta p'\rho_g}{p\gamma} \tag{8}$$

Because there is no heat transfer and friction, the gas phase will comply with

$$p\rho_g^{-\gamma_g} = C \tag{9}$$

where γ_g is the ratio of specific heat of gas phase, C is a constant.

If there is a liquid phase of m unit mass in every unit mass of gas phase, this relationship in the two-phase mixture holds:

$$\frac{\rho}{\rho_g} = 1 + m \tag{10}$$

Substitute Eq. (10) to Eq. (9):

$$p\rho^{-\gamma_g} = C' \tag{11}$$

It can be seen from Eq. (11) that the ratio of specific heat is identical for the mixture and gas phase under isentropic conditions.

Combining the Eqs. (4–8), the following is obtained:

$$\overline{\Delta p}' = \frac{M l_R}{\Delta p S} s\left(\frac{\beta\rho_g\Delta p}{\rho p_2}\frac{\overline{\Delta p}'}{\gamma} + \frac{\dot{m}_l}{Sv\rho_l}\overline{\dot{m}}_l'\right) \tag{12}$$

Thus, the transfer function of the liquid mass flow rate fluctuation to the pressure drop in the recessed chamber can be expressed as

$$\Pi_R = \frac{\overline{\Delta p}'}{\overline{\dot{m}}_l'} = \frac{sMl_R\dot{m}_l\rho\gamma p_2}{[S\rho\gamma p_2 - sMl_R\beta\rho_g]S\rho_l\Delta p v} \tag{13}$$

B. Dynamic Model of a Gas–Liquid Coaxial Swirl Injector

The motivation of this section is to deduce the transfer function for the entire coaxial swirl injector by combining the transfer function of the recessed chamber and the liquid injector.

Because the flow in the recessed chamber is assumed to be homogeneous (analogous to the two-phase flow passing through an orifice plate), the relation between the pressure drop and the mixture mass flow rate is [18,19]

$$\Delta p = \frac{M^2}{2\rho C_t^2\varepsilon_t^2 A_0^2} \tag{14}$$

where C_t is the discharge coefficient when the two-phase mixture flowing through the orifice plate, ε_t is the expansion factor of the mixture, A_0 is the area of the orifice. Similar to the mixture flow in the recessed chamber, C_t and ε_t are set to be one, the following equation holds:

$$\tilde{M} = S\sqrt{2\Delta\tilde{p}\cdot\tilde{\rho}} \tag{15}$$

Where the tilde $\sim$ indicates the fluctuation parameter, and it can be expressed as the sum of steady value and perturbation value, i.e.,

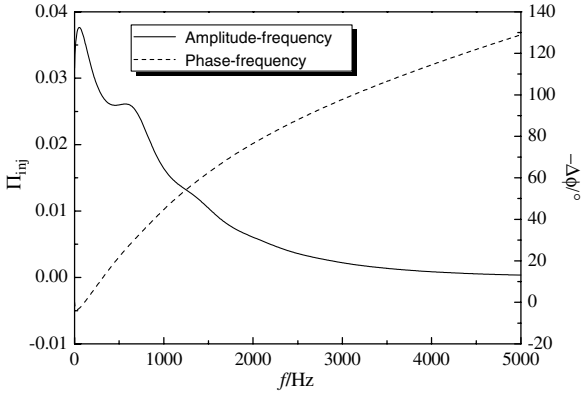

Fig. 5 Dynamics of a liquid swirl injector.

$$\left.\begin{aligned}\tilde{M} &= M + M'\\ \Delta\tilde{p} &= \Delta p + \Delta p'\\ \tilde{\rho} &= \rho + \rho'\end{aligned}\right\} \tag{16}$$

Substituting Eq. (16) to Eq. (15), linearizing it and omitting the high-order quantity, Eq. (15) changes to

$$M' = S^2(\rho\Delta p' + \Delta p\rho')/M \tag{17}$$

Because the liquid is assumed to be incompressible, the variation of density is only caused by the variation of gas density, and Eq. (8) is used again, i.e.,

$$\rho' = \beta\rho'_g = \frac{\Delta p'\beta\rho_g}{p\gamma} \tag{18}$$

The relationship between the relative perturbation quantity of mixture mass flow rate and that of the pressure drop in recessed chamber is

$$\bar{M}' = \Delta\bar{p}'(\rho + \beta\rho_g\Delta p/p_2\gamma)S^2\Delta p/M^2 \tag{19}$$

From Eq. (13), the following can be derived:

$$\overline{\Delta p}' = \Pi_R \cdot \overline{\dot{m}}'_l \tag{20}$$

where $\overline{\dot{m}}'_l$ is the relative perturbation of the flow rate of liquid swirl injector. According to the liquid injector dynamics theory [12], $\overline{\dot{m}}'_l = \Pi_{inj} \cdot \bar{p}'_{inj}$, where Π_{inj} is the transfer function of liquid swirl injector; $\bar{p}'_{inj}$ is the relative perturbation of pressure at the liquid swirl injector inlet. For a convergent nozzle swirl injector,

$$\Pi_{inj} = \frac{\bar{R}^2_{BX}}{a}\frac{\Pi_c\Pi_{k.cII}\Pi_T}{2\Pi_T(\Pi_{k.3II} + \Pi_{k.3III}) + 1} \tag{21}$$

Where Π_T is a complex transfer function of the tangential channel, $\Pi_{k.cII}$ and Π_c are the transfer functions of the vortex chamber and spout nozzle, respectively, $\Pi_{k.3II}$and $\Pi_{k.3III}$ are the complex transfer functions of the vortex chamber, which correspond to the two mechanisms of disturbance propagation from the tangential channel to the vortex chamber. A more thorough description is given by [12]. Many investigators [20–22] have used Eq. (21) to study the dynamics of a liquid swirl injector. Figure 5 shows the typical dynamic characteristics of a liquid swirl injector. It can be seen that the nondimensional amplitude of flow pulsation decreases and the phase contrast increases with the increase of pulsation frequency. Moreover, the undulation on the amplitude-frequency curve is caused by the reflected wave in the swirl chamber.

By combining Eqs. (13), (19), and (20), the transfer function of a gas–liquid coaxial swirl injector can be obtained, as follows:

$$\Pi = \bar{M}'/\bar{p}'_{inj} = \Pi_R\Pi_{inj}(\rho + \beta\rho_g\Delta p/\gamma p_2)S^2\Delta p/M^2 \tag{22}$$

From Eq. (22) it can be seen that the injector configuration parameters (such as recessed length, recessed diameter), working conditions (such as two-phase mass flow rate, mixing ratio, and property of the propellant), all influence the entire injector transfer function; therefore the effect of these parameters on the dynamics of a gas–liquid coaxial swirl injector will be discussed.

III. Results and Discussion

The parameters of the baseline injector are as follows: the length and diameter of the recessed chamber are 24 and 7.3 mm; d_o, d_k, and d_t are 5.7, 8, and 1.6 mm, respectively. The mass flow rate and mixing ratio of the injector are 0.18 kg/s and 8. The number of the tangential inlet n equals 1. A is defined as the geometric parameter of the liquid swirl injector, which can be expressed as [23]

$$A = \frac{(d_k - d_t)d_o}{nd_t^2} \tag{23}$$

The propellant is LOX, and gaseous hydrogen, whose properties are shown in Table 1. In this calculation, the steady pressure drop of the recessed chamber should be given first. In [25], the pressure drop of the recessed chamber is 0.15 MPa when the mixing ratio O/F is six. In the current research, the order of magnitude of pressure drop in recessed chamber is set to be 0.1 MPa for simplicity.

A. Effect of Mixing Ratio

The mixing ratio is defined as the ratio of mass flow rate of the LOX and hydrogen. The baseline injector parameters are taken as the basic geometry, and four different mixing ratios are calculated. Figure 6 shows the results. Figure 6a is the amplitude-frequency diagram, and Fig. 6b is the phase-frequency diagram. It can be seen from the amplitude-frequency diagram that the amplitude response of the fluctuation of two-phase mixture mass flow rate demonstrates a trend of increasing first, and then decreasing in general, as the pulsation frequency increases. At some frequency point (f_1, f_2, f_3, etc., in Fig. 6), there are spikes of amplitude response. According to the literature [8,9], there exists self-pulsation phenomena in a recessed coaxial swirl injector. The frequency at which a sharp increase in the amplitude response is found is considered to be a self-pulsation frequency. When a weak disturbance occurs in the injector, it is composed of every monochromatic component with different frequencies and wavelengths, according to the dispersed wave theory. Just these components whose frequency equals f_1, f_2, etc., would be amplified and cause the occurrence of self-pulsation.

It is believed that this fluctuation frequency response was generated by the coupling of the recessed chamber and the liquid swirl injector. In Fig. 5 small undulations can be seen at the frequency of about 600 Hz and 1300 Hz. In Bazarov's theory of injector dynamics [26], these undulations were caused by the reflected wave in the swirl chamber. The recessed chamber and the liquid swirl injector can form a time lag feedback. Through this feedback, these undulations may be amplified. Hence, the fluctuating frequency response presents the results, as shown in the calculation results.

Moreover, it can be seen from Fig. 6 that the mixing ratio has great effect on the amplitude-frequency characteristics: the mixing ratio is larger, the amplitude response is greater, and the self-pulsation frequencies do not vary with the mixing ratio. Im and Yoon [9], pointed out that the frequency of the spray oscillation by self-pulsation without gas effects matches the frequency of the dominant wave of the liquid sheet, and this frequency is shifted slightly by the

Table 1 Injector flow, fluid properties

Element[a]	Combustion chamber pressure, MPa	Temperature, K	Density, kg/m^3
O_2	10.1	100	1119
H_2	10.1	150	15.4

[a]Critical properties of O_2: $p_c = 5.04$ MPa and $T_c = 155$ K. Critical properties of H_2: $p_c = 1.30$ MPa and $T_c = 33.2$ K [24].

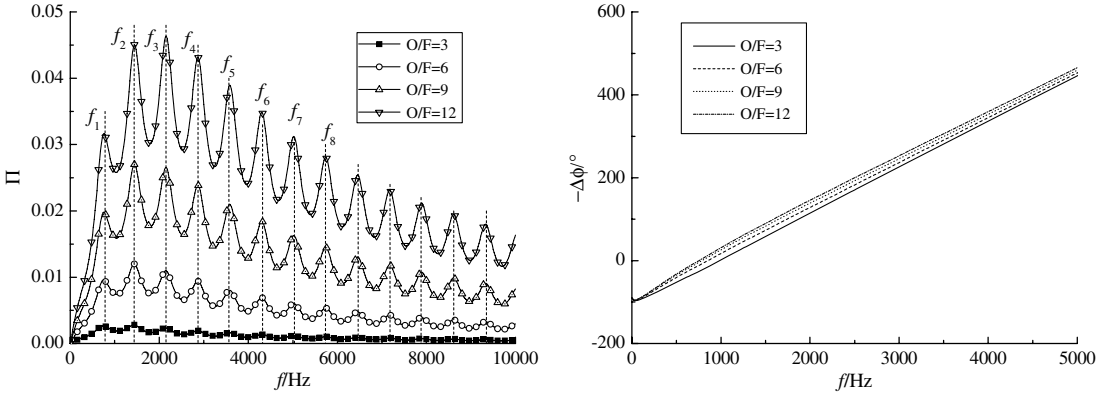

a) Amplitude-frequency characteristics **b) Phase-frequency characteristics**

Fig. 6 Dynamics of coaxial injector with different mixing ratio.

effects of the annular gas. Because the oscillation wave on the liquid sheet depends mainly on the liquid swirl injector, the mixing ratio has little effect on the self-pulsation frequency.

It can be seen from the phase diagram that the phase contrast between the flow rate pulsation and pressure pulsation increases linearly as the pulsation frequency increases. As the mixing ratio increases, the phase contrast increases. However, the influence of the mixing ratio on the phase-frequency characteristics is small. The phase contrast occurs because the propagation speed of a pulsation wave in a two-phase mixture with different mixing ratios is distinct.

B. Effect of Mass Flow Rate

Taking the baseline injector parameter as the basic geometry, the effect of two-phase mass flow rate on the coaxial swirl injector dynamics is analyzed.

Figure 7 shows the dynamics of the gas–liquid coaxial swirl injector with four different mass flow rates. Similarly, the amplitude response presents the trend of increasing first, then decreasing in general, and the phase contrast increases as the pulsation frequency increases. A sharp and narrow increase of the amplitude response occurs at certain frequencies. Furthermore, as the mass flow rate increases, the amplitude response and the phase contrast both decrease. The influence of the mass flow rate on the phase-frequency characteristics is minor.

The literature [8], reported that the model injectors tested at atmospheric antipressure showed that injectors with decreased propellant mass flow have a self-pulsating flow regime in a somewhat wide range of pressure drops of gas and liquid, accompanied by pressure pulsations in a test chamber, gas manifold and liquid feed line, coincident with this analysis. As the injector dynamics theory depicts, the amplitude response increases while the propellants mass flow rate decreases, so self-pulsation is easier to observe than pulsation under larger mass flow rate.

C. Effect of Recessed Length

To investigate the effect of the recessed chamber length on the dynamics of the coaxial injector, injectors with four different recessed chamber lengths are calculated. The inner liquid swirl injectors are recessed at 5, 10, 15 and 20 mm, which correspond to 0.7, 1.4, 2.1 and $2.8d_R$, respectively.

Figure 8 shows the dynamics of the coaxial swirl injector with different recessed lengths. It shows that the amplitude response increases and the phase contrast decreases as the recessed length increases. This conclusion also agrees with the experimental results reported in [9]. Their experiments showed that self-pulsation is not observed with a short recess length, but as the recess length increases, self-pulsation is detected. The increased recess length quickens the occurrence of self-pulsation under the same injection conditions.

D. Effect of Ambient Pressure

Figure 9 shows the effect of ambient pressure on the dynamics of a coaxial swirl injector. The ambient pressures are 6, 8, 10.1 MPa. The amplitude-frequency diagram shows that as the ambient pressure increases, the relative amplitude of mass flow rate pulsation and the phase contrast both decrease; this complies with the phenomenon observed in the experiments [9]. Self-pulsation can be observed in many cases at the ambient pressure of 0.1 MPa; however, self-pulsation is detected only when gas velocity is high at the ambient pressure of 0.5 MPa. A further increase in ambient pressure leads to the suppression of self-pulsation. Moreover, the ambient pressure does not change the self-pulsation frequency.

E. Effect of Geometric Parameters of the Liquid Swirl Injector

As described in Sec. III.A, there is a relationship between the self-pulsation frequency and the dominant frequency of the unstable waves on the liquid film. Thus, it can be deduced that the variation of

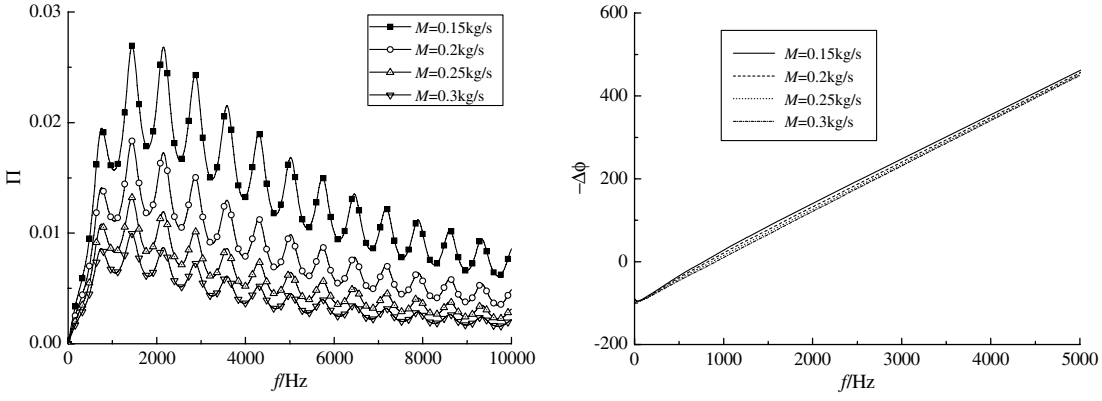

a) Amplitude-frequency characteristics **b) Phase-frequency characteristics**

Fig. 7 Dynamics of coaxial injector with different mass flow.

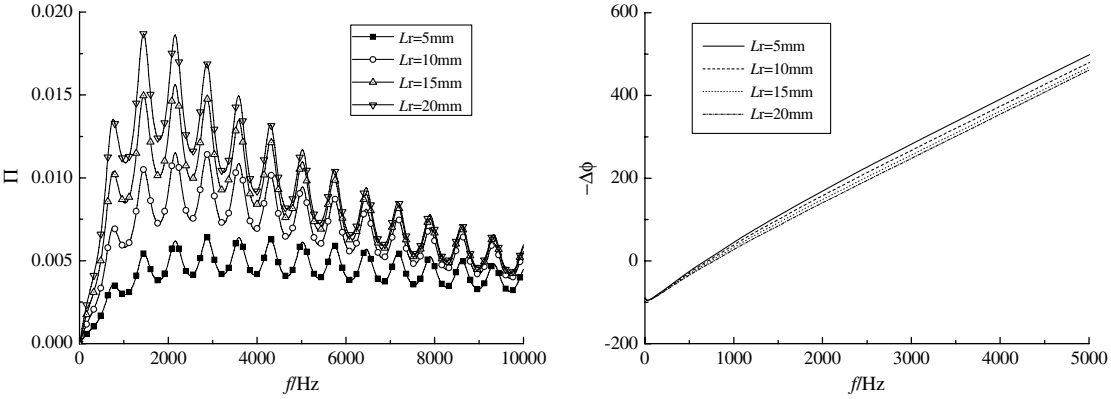

a) Amplitude-frequency characteristics b) Phase-frequency characteristics

Fig. 8 Dynamics of coaxial injector with different length recessed chamber.

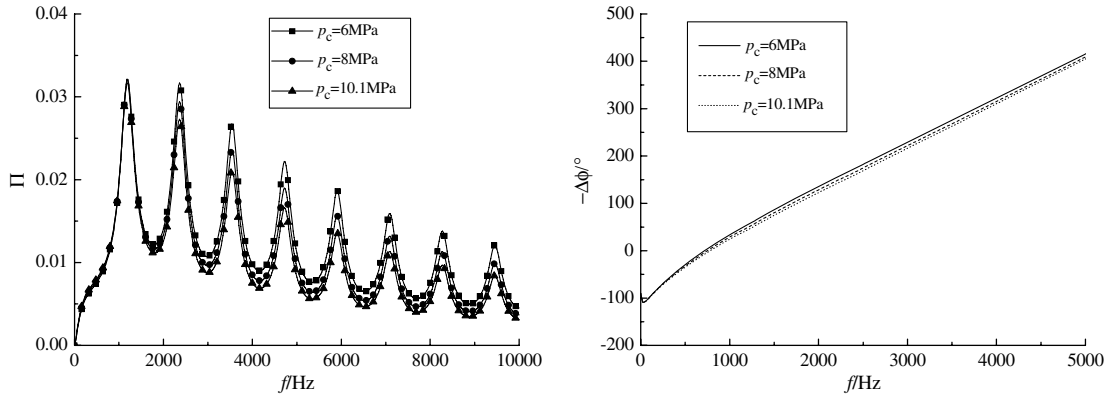

a) Amplitude-frequency characteristics b) Phase-frequency characteristics

Fig. 9 Dynamics of coaxial injector with different ambient pressure.

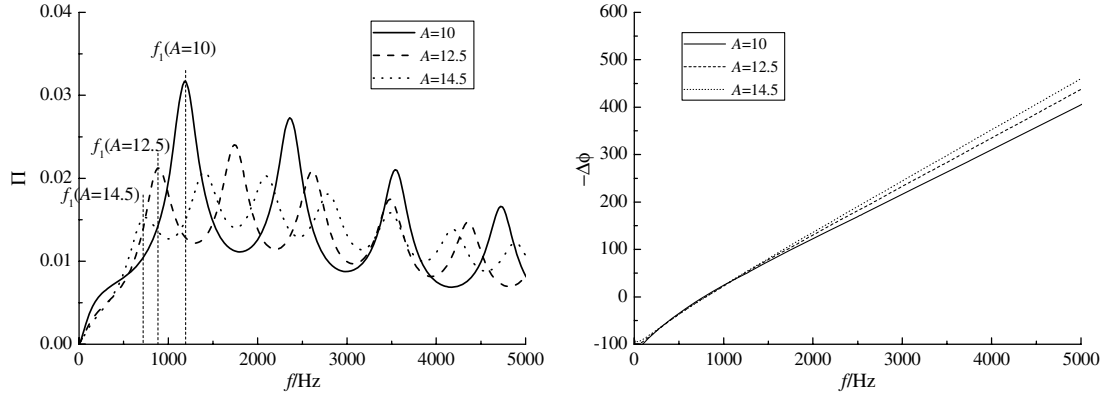

a) Amplitude-frequency characteristics b) Phase-frequency characteristics

Fig. 10 Dynamics of coaxial injector with different geometric parameter *A*.

liquid swirl injector geometry would cause variation of the liquid film in the swirl injector and the waves on the liquid film, further leading to variation of the self-pulsation frequency of the gas–liquid coaxial swirl injector. Here we investigate the effect of liquid swirl injector configuration on the dynamics of the coaxial injector by changing the geometric parameter of the liquid swirl injector *A* from 10 to 14.5.

Figure 10 shows the calculated results. It can be seen from the amplitude diagram that the amplitude response decreases as the liquid swirl injector's geometric parameter *A* increases. This is because *A* denotes the swirl intensity of the liquid sheet. Increasing *A* causes the liquid flow area to decrease. A smaller liquid flow area decreases the collision of the liquid and gas phase, further decreasing the self-pulsation amplitude. Moreover, increasing *A* would decrease the amplitude of the liquid mass flow rate pulsation according to the liquid swirl injector dynamics theory, further decreasing the amplitude of the two-phase mixture mass flow rate.

Furthermore, with the increase of *A*, pulsation frequency decreases. As shown in Fig. 6, the first self-pulsation frequency decreases from 1192 to 719 Hz. The phase-frequency diagram shows that the phase contrast increases somewhat as *A* increases.

IV. Conclusions

A theoretical model of the linear dynamics of a gas–liquid coaxial swirl injector was developed. The model considers the influence of the liquid phase only, and divides the dynamic process of the coaxial

swirl injector into two parts: the flow in the liquid swirl injector and the flow in the recessed chamber. The linear transfer function of the recessed chamber was deduced based on fundamental fluid mechanics equations. The transfer function of the entire gas–liquid coaxial swirl injector was obtained by combining the transfer function of the recessed chamber and the liquid swirl injector. The transfer function depicts the characteristics of the coaxial swirl injector in the frequency domain. Based on the deduced transfer function, the influences of the configuration parameters on the injector dynamics were calculated. The qualitative trend of the predicted dynamics agrees reasonably well with the observations reported in the literature. The effects of the parameters were analyzed and the conclusions were obtained as follows:

1) The amplitude response of the fluctuation of two-phase mixture mass flow rate demonstrates a trend of increasing first, and then decreasing in general, as the pulsation frequency increases. The phase contrast between the relative pulsation of mass flow rate and injection pressure increases linearly as the pulsation frequency increases.

2) At some frequency point, spikes of amplitude response occur, which are considered to be the self-pulsation frequency, and the self-pulsation frequency does not vary with other configuration parameters or working conditions, except the geometric parameter of the liquid swirl injector. With the increased geometric parameter, the self-pulsation frequency decreases.

3) A smaller mixing ratio, larger mass flow rate, higher ambient pressure, smaller ratio of recess length-to-diameter, and larger geometric parameter, would all serve to decrease the amplitude response of the mass flow rate pulsation. But these parameters have little effect on the phase frequency of the coaxial swirl injector.

Acknowledgments

The financial support of China National Nature Science Funds (Support number: 50406007) and the Innovation Foundation of Beijing University of Aeronautics and Astronautics for Ph.D. Graduates is gratefully acknowledged.

References

[1] Gill, G. S., "Liquid Rocket Engine Injectors," NASA SP-8089, 1976.
[2] Inamura, T., Miyata, K., Tamura, H., and Sakamoto, H., "Spray Characteristics of Swirl Coaxial Injector and its Modeling," AIAA Paper 2001-3570, 2001.
[3] Cohn, R. K., Strakey, P. A., Bates, R. W., Talley, D. G., Muss, J. A., and Johnson, C. W., "Swirl Coaxial Injector Development," AIAA Paper 2003-125, 2003.
[4] Tharakan, T. J., and Gupta, N. K., "Effect of Recess on the Spray Characteristics of Gas–Liquid Coaxial Swirl Injectors," *Proceedings of the International Conference on Aerospace Science and Technology*, Bangalore, India, 2008.
[5] Soller, S., Wagner, R., Kau, H., Martin, P., and Mäding, C., "Combustion Stability Characteristics of Coax-Swirl-Injectors for Oxygen/Kerosene," AIAA Paper 2007-5563, 2007.
[6] Zhang, M., Wang, L., Zhang, Z., and Yang, G., "Flame Characteristic Test Study of Coaxial-Swirl Injector," *Combustion Science and Technology*, Vol. 14, No. 1, 2008, pp. 1–5.
[7] Yang, L., Ge, M., Zhang, M., Fu, Q., and Cai, G., "Spray Characteristics of a Recessed Gas–Liquid Coaxial Swirl Injector," *Journal of Propulsion and Power*, Vol. 24, No. 6, 2008, pp. 1332–1339. doi:10.2514/1.23977
[8] Bazarov, V., "Self-Pulsations in Coaxial Injectors with Central Swirl Liquid Stage," AIAA Paper 1995-2358, 1995.
[9] Im, J.-H., and Yoon, Y., "The Effects of the Ambient Pressure on Self-Pulsation Characteristics of a Gas/Liquid Swirl Coaxial Injector," AIAA Paper 2008-4850, 2008.
[10] Andreyev, A. V., and Bazarov, V. G., *Dynamics of Gas–Liquid Injectors*, Mashinostroenie, Moscow, 1991 (in Russian).
[11] Andreyev, A. V., and Chepkin, V., "Autovibration of Coax Injector Elements of O_2/H_2 Staged Combustion Liquid Rocket Engines," AIAA Paper 1995-2837, 1995.
[12] Bazarov, V., and Yang, V., "Liquid-Propellant Rocket Engine Injector Dynamics," *Journal of Propulsion and Power*, Vol. 14, No. 5, 1998, pp. 797–806. doi:10.2514/2.5343
[13] Sasaki, M., Sakamoto, H., Takahashi, M., and Tomita, T., "Comparative Study of Recessed and Non-Recessed Swirl Coaxial Injectors," AIAA Paper 1997-2907, 1997.
[14] Nunome, Y., Tamura, H., Onodera, T., Sakamoto, H., Kumakawa, A., and Inamura, T., "Effect of Liquid Disintegration on Flow Instability in a Recessed Region of a Shear Coaxial Injector," AIAA Paper 2009-5389, 2009.
[15] Luo, Z., *Fluid Network Theory*, China Machine Press, Beijing, 1988, p. 207 (in Chinese).
[16] Harrje, D., and Reardon, F., "Liquid Propellant Rocket Combustion Instability," NASA SP-194, 1972, p. 108.
[17] Feiler, C. E., and Heidmann, M. F., "Dynamic Response of Gaseous-Hydrogen Flow System and its Application to High-Frequency Combustion Instability," NASA TN D-4040, 1967.
[18] Yan, C., *Gas–Liquid Two Phase Flow*, Harbin Engineering Univ. Press, Harbin, China, 2010 (in Chinese).
[19] Upp, E. L., and LaNasa, P. J., *Fluid Flow Measurement, A Practical Guide to Accurate Flow Measurement*, Gulf Professional, Woburn, MA, 2002.
[20] Fu, Q., Yang, L., and Wang, X., "Theoretical and Experimental Study of the Dynamics of a Liquid Swirl Injector," *Journal of Propulsion and Power*, Vol. 26, No. 1, 2010, pp. 94–102. doi:10.2514/1.44271
[21] Seo, S., Kim, S., and Choi, H., "Combustion Dynamics and Stability of a Fuel-Rich Gas Generator," *Journal of Propulsion and Power*, Vol. 26, No. 2, 2010, pp. 259–266. doi:10.2514/1.46568
[22] Ismailov, M., and Heister, S., "Nonlinear Modeling of Classical Swirl Injector Dynamics," AIAA Paper 2009-5402, 2009.
[23] Bayvel, L., and Orzechowski, Z., *Liquid Atomization*, Taylor and Francis, Washington, D.C., 1993.
[24] Oefelein, J. C., "Thermophysical Characteristics of Shear-Coaxial LOX-H_2 Flames at Supercritical Pressure," *Proceedings of the Combustion Institute*, Vol. 30, No. 2, 2005, pp. 2929–2937. doi:10.1016/j.proci.2004.08.212
[25] Sun, J., Zhuang, F., and Wang, J., "Effects of Recess on Coaxial Injector's Discharge Coefficient and Performance," *Journal of Propulsion Technology*, Vol. 24, No. 5, 2003, pp. 452–455.
[26] Bazarov, V., *Dynamics of Liquid Injectors*, Mashinostroenie, Moscow, 1979 (in Russian).

D. Talley
Editor-in-Chief